ADVANCED FUNCTIONAL MATERIALS
www.afm-journal.de

Tunable Flexible Pressure Sensors using Microstructured Elastomer Geometries for Intuitive Electronics

*Benjamin C.-K. Tee, Alex Chortos, Roger R. Dunn, Gregory Schwartz, Eric Eason, and Zhenan Bao**

Pressure and touch sensitivity is crucial for intuitive human-machine interfaces. Here, we investigate the use of different microstructured elastomers for use as dielectric material in capacitive pressure sensors. We use finite element modeling to simulate how different microstructures can reduce the effective mechanical modulus. We found that pyramidal structures are optimal shapes that reduce the effective mechanical modulus of the elastomer by an order of magnitude. We also investigate the dependence of spacing of the pyramidal microstructures and how it impacts mechanical sensitivity. We further demonstrate the use of these elastomeric microstructures as the dielectric material on a variety of flexible and stretchable substrates to capture touch information in order to enable large area human-computer interfaces for next generation input devices, as well as continuous health-monitoring sensors.

1. Introduction

There is an increasing interest and demand for large area, flexible and stretchable electronic skins for assistive robots and wearable electronics.[1] One of the important application of electronic skins is the ability to sense human interaction seamlessly.[1–3] In humans, the skin contains different types of touch receptors in order to respond to varying types and degrees of mechanical forces. For example, the Ruffini's corpuscles has differentiated nerve endings that senses sustained forces, while the Pacinian corpuscles respond with higher sensitivity to lower (<100 Pa) vibrational forces.[4] The human's skin touch sensitivity is truly remarkable, and recreating the ability to sense force magnitudes in artificial systems could provide seamless interaction with robots or digital electronics. For example, current smartphone touchscreens and laptop trackpads can detect the position of fingers accurately, but cannot sense how much force users apply. Having such pressure information could enable more intuitive human-computer interactions such as pressure-gesture driven interfaces for future flexible or stretchable natural, mobile computing devices. For wearable electronics, having a flexible or stretchable pressure sensor on a device such as a watch can be useful for two reasons: (i) non-invasive monitoring of blood pressure if the sensor is sensitive enough to pick up pulsations from the radial artery,[5,6] and (ii) as pressure-based user input interfaces.

There are several types of artificial force sensing technologies that transduce an external force into a signal that can be read digitally.[7,8] Resistive based pressure sensors rely on conductive polymer composites that modulate the resistivity by displacement of conductive fillers in an elastic polymer.[8,9] When pressure is applied, the inter-particle spacing between the conductive fillers decreases, enhancing electron tunneling and thereby lowering the effective resistance. At higher pressures, the conductive particles reach percolation and the resistance decrease begins to reach an asymptotic value that depends on the intrinsic conductivity of the particles. The resistance change with pressure of such resistive sensors is typically highly nonlinear, and changes by several orders of magnitude.[10] Someya et al. used such piezo-resistive sensors in an array of organic field effect transistors as readout elements for large area pressure sensitive skin, achieving detection thresholds of about 10 kPa.[11] Recently, they have further improved the sensitivity to detect less than 10 kPa using higher performance organic semiconductors on extremely thin plastic foils.[12] Kim et al. used ultra-thin elastomer as a substrate with piezo-resistive sensors for ultra-conformal sensors, which can be laminated easily onto surfaces of organs.[13] Takei et al. used carbon nanotubes transistors with better transconductance to enhance sensitivity and response time of such pressure sensors.[14] Other types of pressure sensors include piezo-electric and ferro-electric sensors that generate a transient voltage in response to dynamic

Prof. Z. Bao
Chemical Engineering Department
381 North South Axis, Rm 213
Stanford 94305, USA
E-mail: zbao@stanford.edu
Dr. B. C.-K. Tee
Electrical Engineering Department
Packard Building
Stanford 94305, USA
Dr. G. Schwartz
Chemical Engineering Department
381 North South Mall
Stanford 94305, USA
A. Chortos, R. R. Dunn
Material Science and Engineering Department
Stanford 94305, USA
E. Eason
Mechanical Engineering Department
Stanford 94305, USA

DOI: 10.1002/adfm.201400712

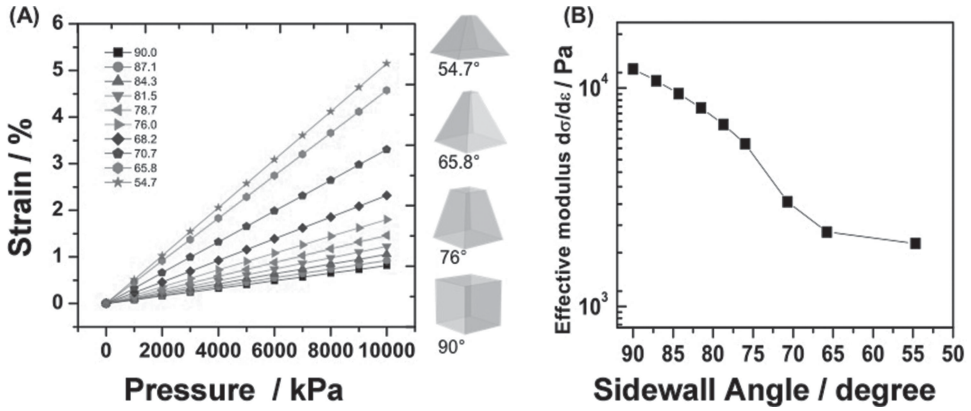

Figure 1. Simulation data showing A) predicted stress-strain relationship of different sidewall angled microstructures and B) predicted effective modulus of the microstructures showing almost one order of magnitude decrease as sidewall angle decreases.

pressure changes.[15,16] Another novel type of mechanical sensor that can also be used as an actuator is the liquid crystalline elastomers.[17] It is also possible to use optical methods to interrogate elastic polymer waveguides[18] for transparent, tactile sensitive displays.

All of these mechanical sensors rely on an important prerequisite: the compressibility of the material that is directly in contact with the force applied. The greater the compressibility of the material used, the greater the sensitivity of the sensor will be. Furthermore, depending on the type of application, different sensitivities might be required, just like how human skin uses different receptors for different types of forces. Therefore, it is important to be able to manufacture materials with tunable mechano-sensitivity. Recently, we have made a new type of pressure sensors using microstructured elastomer as gate dielectric material in organic transistors.[19] In this work, we study the geometrical dependence of the microstructures on mechanical sensitivity. We further present the use of soft PDMS molds to replicate the microstructures and test their electro-mechanical response to pressure. We next demonstrate two possible applications of these microstructured elastomer capacitive pressure sensors.

For parallel-plate capacitive sensors, the equation governing the capacitance per unit area is given by

$$C = \frac{\varepsilon_r \varepsilon_0}{d} \quad (1)$$

where ε_r is the relative dielectric constant of the material, ε_0 is the permittivity of free space, and d is the electrodes separation, ignoring fringe electric fields. From Equation (1), two factors affect the capacitance, (i) the relative dielectric constant of the material, and (ii) the electrode separation. Any mechanical force that affects either of the above parameters will change the capacitance; and in this way, we can determine the force based on a pre-determined force-capacitance calibration of the sensor device. In order for high sensor sensitivity, which is required for good signal to noise ratios (SNR), it is important that the mechanical compressibility of the dielectric material is high so that a small applied force can decrease d significantly. However, the material needs to also have a fast mechanical response in order to return to its original shape and size quickly in time for the next force stimulus. Therefore, elastomers with fairly low viscoelasticity are ideal materials for the dielectric layer. Furthermore, elastomers are inherently flexible and suitable for use in flexible electronic devices. For example, Metzger et al. have used polyolefin foams as a compressible dielectric material for measuring forces to target smart shelf applications to detect objects.[20] In order to have high mechanical sensitivity, however, a low mechanical modulus is required for high mechanical sensitivity. Elastomers such as PDMS (Sylgard 184) typically have a modulus of ~2 MPa.[21] Elastomers with smaller modulus also tend to exhibit greater viscoelasticity, which affects the sensor's time response. Previously, we found that thin unstructured PDMS films (<10 μm) exhibit high viscoelasticity.[19] Therefore, we employed the strategy of structuring the elastomer in such a way that adds air gaps in an orderly fashion within the elastomer layer.[5,19] In this manner, we can obtain different sensitivities by using pre-determined structural geometries and their spatial locations. Here, we further studied how the type of geometries and spatial arrangement affects the mechanical sensitivity of the microstructures. We also performed finite element modeling to get a first-order understanding of the structure-property relationship.

2. Results and Discussion

2.1. Finite-Element Modeling

As we discussed, there are a multitude of shapes that can be used to structure the elastomer dielectric layer. In order to attain an understanding of the relative effects, we performed a finite element modeling and simulation with different geometrical shapes. **Figure 1**a shows a simulation of some possible 3-dimensional shapes and their corresponding compressibility. In our simulation, the heights of the structures are kept constant while the sidewall angles with respect to the base were varied. We observe that moving from a square cross-section to a trapezoidal cross-section with sloping sidewalls gives a higher slope in the stress-strain curve, which implies that a smaller force decreases the electrode separation more compared to a square cross-section. In other words, the greater the angle of the slope defined by the perpendicular sidewall to the base sidewall, the greater the sensitivity of the geometrical shape

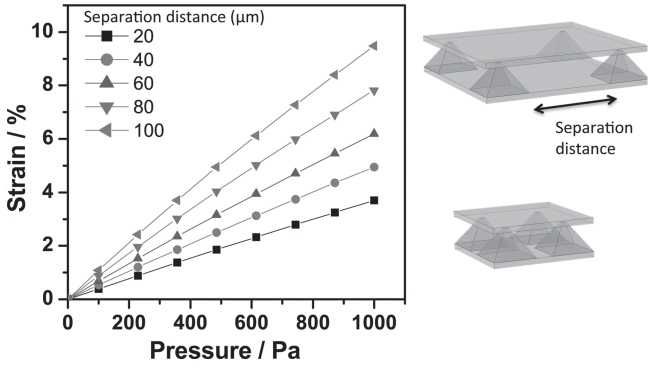

Figure 2. Simulation data of stress-strain relationship with increasing separation of pyramidal microstructures.

to compression. This can be also explained by considering the stress distribution of the different geometrical shapes. In a cube structure, the stress distribution is fairly constant throughout the height of the cube due to the uniform cross-sectional area. However, when the shape is more pyramidal, the stress distribution is non-uniform, and is concentrated at the pointed tips due to the smaller contact area (hence higher stress and consequently strain assuming modulus remains fairly constant), rather than the broad base of the pyramid structure. Thus, the pyramid tips compress more, resulting in the higher mechanical deformations at the top. Therefore, the pyramidal shapes are more sensitive. It is noted that we did not completely taper the top of the pyramidal shapes in our simulations to avoid non-linearity issues associated with very sharp features in the mechanical modeling. The sensitivity decreases as the pyramid top compresses and the structure reverts back to a more cubic cross-sectional area. This effect changes the sidewall profiles of the structure, which affects subsequent compression sensitivity. Figure 1b shows a plot of the effective compressive modulus versus sidewall angle of the structures by taking the inverse slope of the strain versus stress plot in Figure 1a. By simply changing the elastomer geometry via decreasing the sidewall angle, we can decrease the effective compressive modulus by close to an order of magnitude without the need to intrinsically change the chemical structure of the elastomer.

Another design parameter in the sensitivity of such dielectric structures is the spatial arrangement of the structures. In order to study this effect, we created models containing four similar structures with varying spacing between the structures. **Figure 2.** shows how the compressibility of the structures is affected by the placement within a unit area. As the structures are spaced further apart, the compressibility increases. Therefore, changing the spacing of the structures is another way to increase the sensitivity of the dielectric material once the shape of the structure is chosen. One can also consider placing different geometrical structures within the same spatial area for purposes of modifying the range of compression sensitivity. We created one such prototype elastomer layer, which will be described in the later sections.

2.2. Design and Fabrication of the Microstructures

Based on the results of our simulation, we observe that the greater the slope of the sidewalls, the greater the sensitivity. In order to create such pyramidal geometries from elastomers, we used soft lithographic molding technique.[22] We first etch pyramidal pits in (100) silicon wafers using potassium hydroxide (KOH) as an etchant. The resulting pits have a sidewall angle of 54.7° due to the different etch rates in the different silicon crystallographic planes in KOH.[23] The dimensions and positions of the pits were determined by lithographically patterning a silicon dioxide that serves as an etch mask because it has a relatively slow etch rate in KOH. Next, we proceeded to create soft lithography molds out of PDMS using the etched silicon molds as a template. In order to obtain a template that has the same features as the silicon molds, we repeated the PDMS mold making process twice using the first replicated mold as template for the final mold. The use of soft molds facilitates the molding of our elastomer structures onto rigid substrates such as silicon in order to easily characterize the sensitivity of the micro-structures. These processes are illustrated in **Figure 3**. Furthermore, the soft PDMS molds are less prone to drastic failure because of their elastic nature compared to the brittle silicon molds. Using a spincoating process to control the thickness of the residual PDMS layer, we mold the microstructures onto the rigid silicon wafers for electro-mechanical

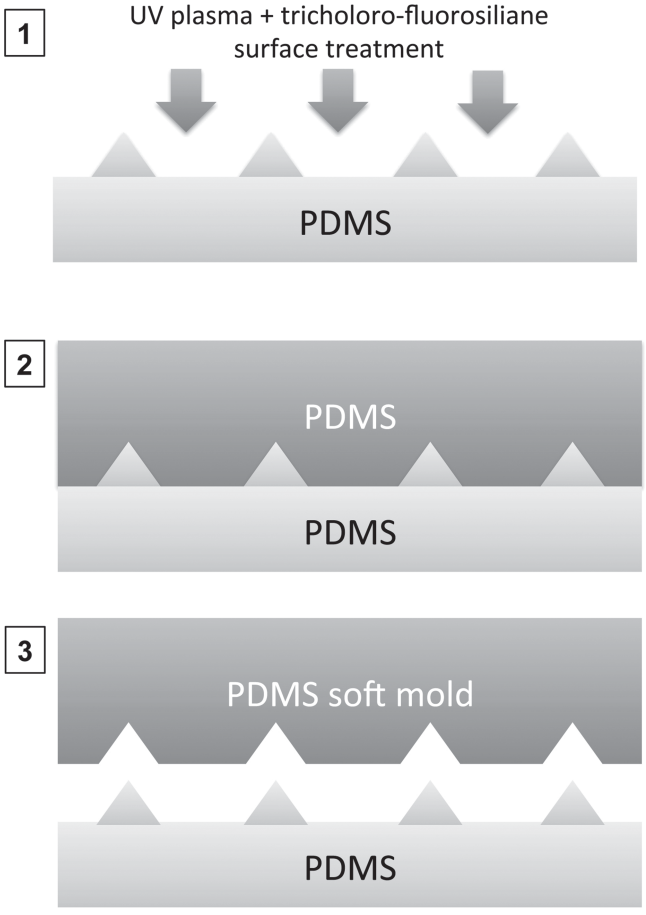

Figure 3. Schematic process for the soft PDMS molds. Step 1: Treat surface of PDMS mold after first feature replication step from silicon. Step 2: Pour PDMS over treated surface of PDMS mold and cure to complete. Step 3: Remove PDMS soft mold and treat the surface again with fluorosilanes to use for subsequent feature replications.

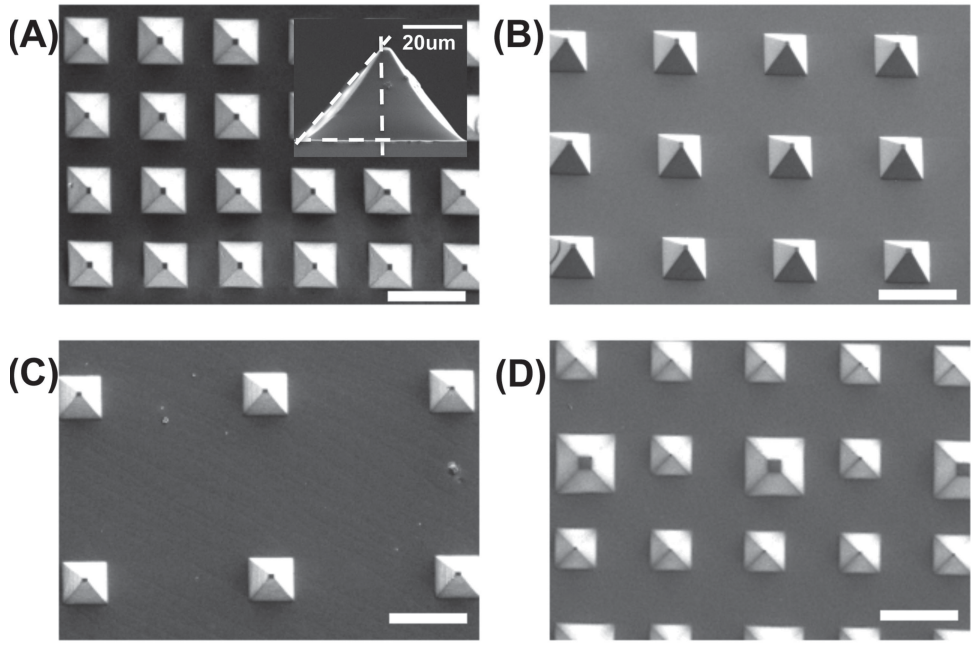

Figure 4. Scanning Electron Microscope (SEM) of different spatial arrangement of pyramidal microstructured PDMS. A) Spacing of 41 μm, B) 88 μm, C) 182 μm and D) interspersed design of two pyramidal structures with different base area (images scale bar 100 μm). Inset in (a) Cross-section SEM of the pyramidal microstructure showing sidewall angle and height. Note that the residual base film height is negligible compared to the pyramidal structure height.

characterization. The PDMS was cured for more than 24 hours at 80 °C, and the mechanical tests were carried out within 24 hours to eliminate potential PDMS aging effects.[24]

From **Figure 4**, we see the resultant different spatial arrangement of the PDMS microstructures. The microstructures have a base of 55 μm and periodic spacing of 41 μm, 88 μm, and 182 μm. Figure 4D shows the interspersed design of two patterns with different microstructures of base length 55 μm and 78 μm. All microstructures have heights of about 34 μm. In our design, we chose 34 μm tall pyramids so that the residual film on the microstructures are significantly thinner (1.5 μm) than the heights of the pyramids (see Figure 4A inset). An additional residual layer that is a small percentage of the microstructure height would not significantly impact the capacitances obtained from such microstructured film. Conversely, if we had used microstructures of smaller heights, then we would have to take into account the compression of the residual film in our characterization. Smaller microstructures have the advantage of higher capacitance per unit area, and are useful for use as gate dielectric of organic transistors.[19] In order to obtain very thin residual films of PDMS, the use of thinners such as hexane was needed in prior work.[19] In this work however, we used PDMS without any additional solvents because of the focus on understanding how different spatial arrangements affects the electromechanics of such microstructures.

2.3. Characterization of Sensor Performance

An automated mechanical test stage was assembled and custom software written to control the characterization of the sensor performance via a computer, as shown in **Figure 5**. The sensor consists of the microstructured dielectric sandwiched between

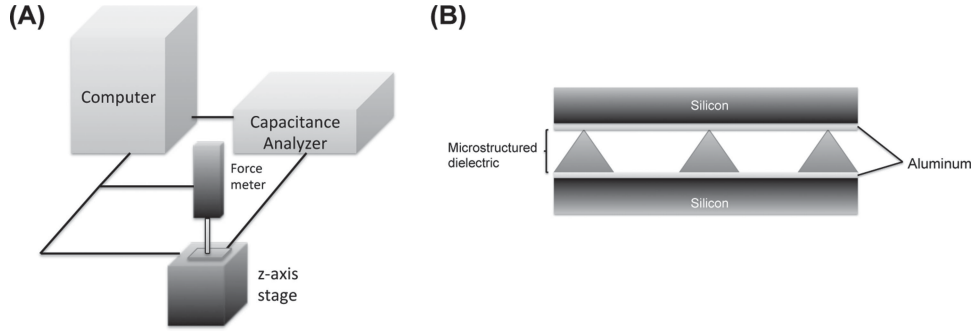

Figure 5. Schematic of characterization setup for microstructured capacitive pressure sensor. A) A computer controls the z-axis stage to apply a force on the device. It records the applied force and capacitance from the sensor device simultaneously. B) Schematic of the sensor structure.

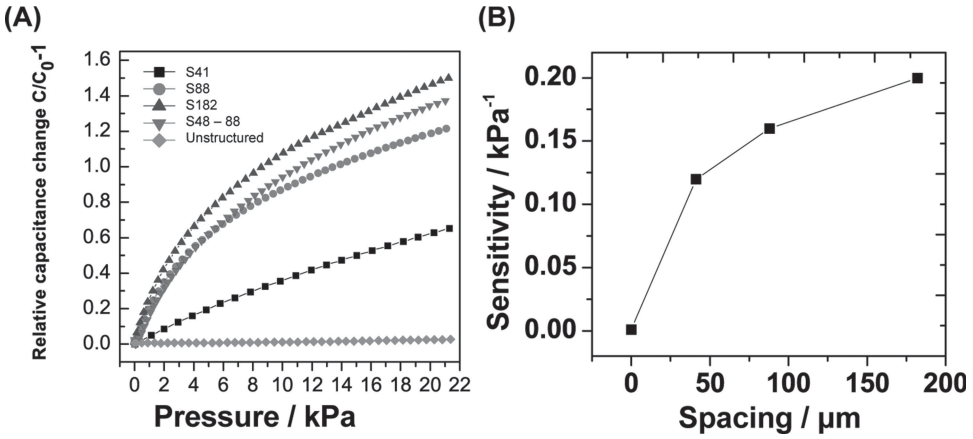

Figure 6. Capacitance change with increasing pressure for different spatial configuration of microstructured PDMS. A) Relative capacitance change with respect to pressure. S41, S88 and S182, corresponding to spacing (edge-to-edge) of 41 µm, 88 µm, and 182 µm respectively. S48–88 refers to the pyramidal arrangement with 48 µm and 88 µm pyramids shown in Figure 3D. B) Sensitivity values plotted with spacing distance of the microstructures for pressure values less than 4 kPa.

two rigid Si substrates coated with aluminum as the electrode as shown in Figure 4B. We chose to use rigid Si substrates instead of flexible substrates in order to avoid non-planarity effects that would affect our study of the structure-property relationship of the PDMS microstructures. Using this sensor structure, we studied different spatial arrangement of the pyramidal microstructures, as well as interspersing different geometrical shapes within the same patterns as shown in Figure 3.

We compared the sensitivity of the different spatial arrangements of the microstructures shown in **Figure 6**. An increasing followed by decreasing ramp force was applied to the microstructures using a silicon wafer coated with aluminum. The capacitance was measured at each incremental load. As expected, we observe that the microstructures with smallest spacing provide the least sensitivity in terms of relative capacitance change from the initial value. From Figure 6, we see that the pattern with pyramids having the smallest spacing (41 µm) was indeed the least sensitive to mechanical compression. This is as we expected from the simulation results. The most sensitive spatial arrangement was from pyramids spaced furthest apart (182 µm). We also note that by incorporating pyramids with a broader base within the spatial arrangement such that each unit cell contains one pyramid of larger base maintains fairly high sensitivity and longer linear initial range. Furthermore, it can also provide a larger contact area for the opposing electrode to adhere to. This dual microstructural pattern demonstrates further the sensitivity tunability of the microstructured dielectric strategy for pressure sensing.

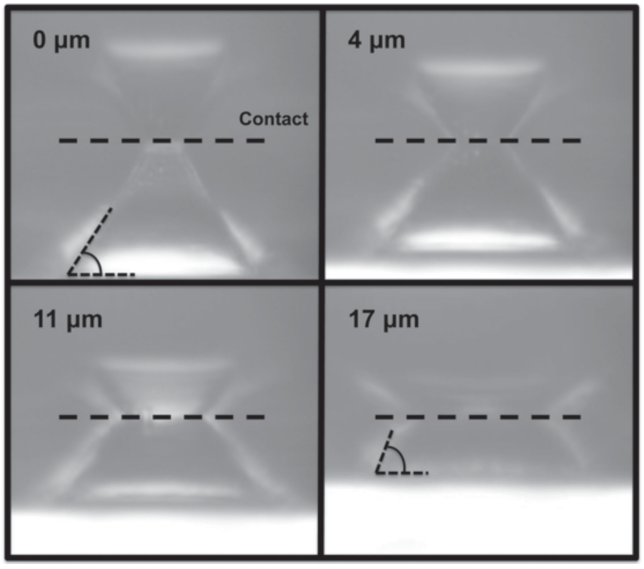

Figure 7. Optical side-view images during compression of the microstructures. The dotted line is where the microstructured PDMS comes into contact with the stationary opposing surface. The bottom substrate is moving upwards to compress the microstructured PDMS. The PDMS is pressed against a clear, transparent acrylic substrate to enable optical imaging.

We further studied the cross-section profile in-situ during compression of the microstructures by optical imaging. From **Figure 7**, the compression profile shows that as the pyramidal structure is compressed, the volume of empty space is filled by the incompressible elastomer (PDMS). Thus the overall volume of PDMS stays constant during compression and takes up the space of the surrounding voids. In a capacitor structure, this increases the volume ratio of dielectric material to air within the gap between the two opposing electrodes, thereby increasing the capacitance in addition to the decreasing electrode spacing.

In addition to measuring capacitance changes during compression, we also recorded the stress-strain relationship during compression. The resulting compression distance normalized by the number of pyramids versus force is shown in **Figure 8**. From the graph, as expected, each pyramid compresses more when they are spaced in a sparser configuration. After the initial compression of about 5 µm, the initial compressibility decreases significantly. This is expected as the top of the microstructure is most sensitive to compression due to its small area. As the area of contact increases, the pressure exerted on the microstructure is reduced, eventually causing the compressibility to reach the bulk modulus of PDMS. This explains why

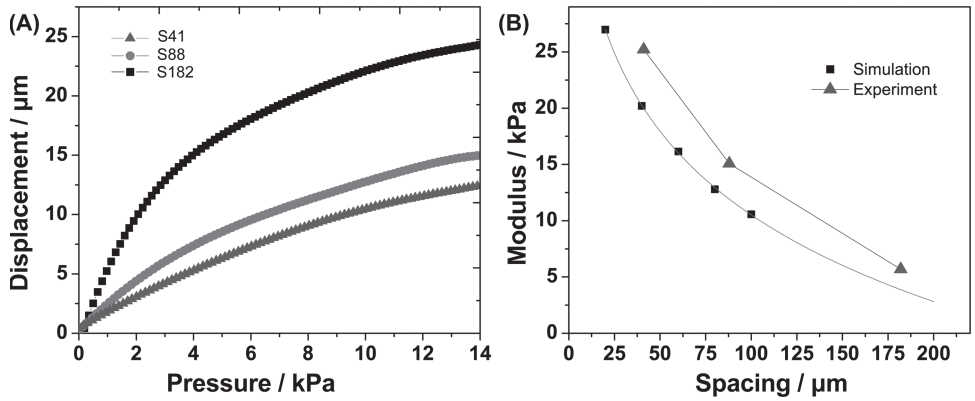

Figure 8. Stress-strain relationship versus simulated results for different spacing of microstructures. A) Fitted experimental data for strain vs. pressure for three spacing. B) Experimental data of the modulus compared to simulation results.

the slope of the curves in Figure 8A tends to reach the same value above 4 kPa.

2.4. Applications

2.4.1. Pulse Monitoring

Wearable electronics has attracted a dramatic increase in interest over the last few years, with several companies introducing smart-watches, smart-wristbands (such as Nike® FuelBand, Fitbit® Flex, MistFit Wearables, etc), and even smart-rings. While the current generation of wearable electronics mainly monitors motion, incorporating health monitors in wearable devices is the next logical step in the evolution of potential impact of wearable electronics. Here, the high sensitivity and fast response time of the microstructured dielectric pressure sensors can be advantageously used for bio-health monitoring and tele-medicine. For example, the pressure sensors can be placed on robotic hands, which can then measure the human pulse and if properly calibrated, blood pressures. In order to assess the feasibility of this application, we molded the microstructures (S88) onto flexible plastic sheets coated with transparent and slightly flexible transparent indium tin oxide (ITO) as electrodes. Previously, we demonstrated that microstructured capacitive sensors coupled with organic transistors can amplify the capacitance change and read pulsations of the radial artery on a human wrist.[5] In this paper, we show that we can use such sensors for detection of pulsations on the human finger tips. **Figure 9** shows the signal from such a capacitive pressure sensor when a human finger was placed on top of the sensor. The sensor output shows a clear pulse waveform from the human finger tip. The captured capacitance change waveform is similar to a photoplethysmograph,[25] which measures changes in blood volume in the finger tip due to the human pulse. Peaks indicating different points in the human pulse can be seen, which are correlated to cardiovascular conditions such as arterial stiffening.[5] The current signal to noise ratio (SNR) from the peak to baseline reading is approximately 8, and can be further improved with optimizations on how the finger is placed on the sensor to enable pulsation capture within the first several kPa, where the capacitive sensor is most sensitive.

2.4.2. Force Sensitive Trackpads

To demonstrate the large area scalability of the capacitive pressure sensors, we molded the pyramidal structures across a large

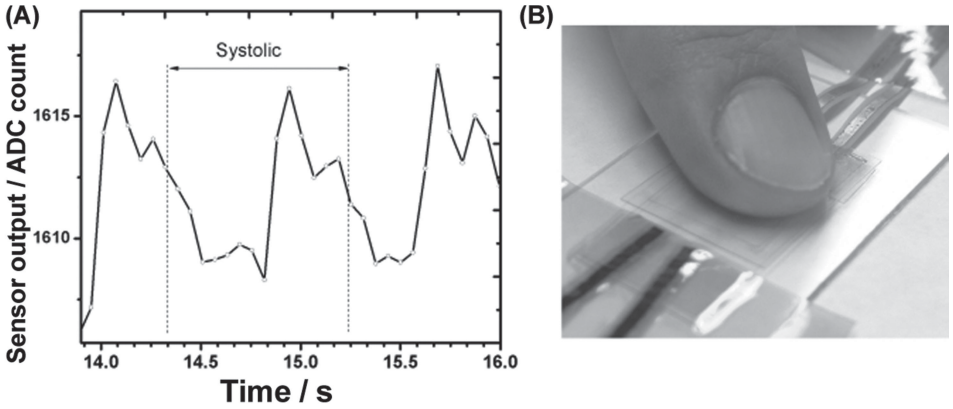

Figure 9. Finger pulse waveform. A) Sensor output. B) Optical image of finger on sensor.

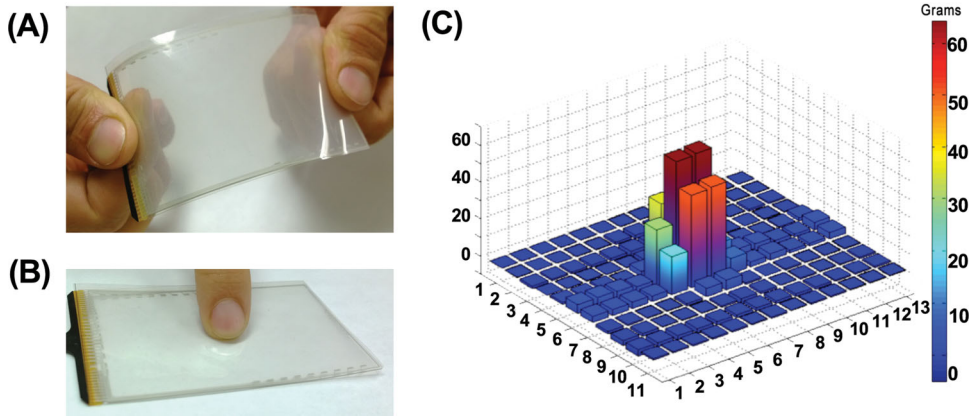

Figure 10. An array of 130 pressure sensor 'pixels' response. A) Flexible sensor sheet. The electrodes were arranged in a cross-bar array with the microstructures sandwiched in between the electrodes. B) Apply pressure on sensor sheet. C) Response of sensor pixels due to applied pressure by finger.

area of 2 cm by 4 cm and integrated it into a cross-bar matrix array of 13 by 10. The sensor sheet comprises of patterned conductive ITO electrodes on top of flexible PET sheets. Each pixel was spaced about 3 mm from each other pixel, with an overlap area of about 2 mm^2. The microstructured dielectric (S88) were sandwiched between the patterned ITO electrodes. Using a capacitive sensing integrated circuit, we successfully measured 130 force sensitive 'pixels'. In **Figure 10**, a small load of 50 grams (about 10 kPa) to the center of the array and Figure 10 shows the output of the array. We observe slight variations of the sensor response in different areas of the film (Supplementary Figure 1). This could be due to variations in the molding manufacturing process for such larger area sensors. The pixel areal variations can be improved with better equipment that control the compression force in the molding over large areas. The load was applied in a hysteretic sweep from 0 to 50 g (10 kPa) and from 50 g to 0 g, and the resulting curves show a small hysteresis, which compares favorably to foam-based capacitive sensors.[20] We expect that the large area force sensors can be useful in future computer trackpads or other input devices (such as computer mice) where force levels in addition to the position of the finger is measured, enabling new computer-user interactions.

3. Conclusions

We have studied the compressibility of PDMS microstructures using finite element models and the effects of spatial arrangements on the mechanical sensitivity of the microstructured films. Furthermore, we have applied these microstructured films as the dielectric layer in a parallel plate capacitor structure as use in pressure sensors. The sensors were demonstrated in various applications such as blood pulse monitoring and next generation force sensing trackpads. The ease of manufacturing, high mechanical sensitivity and low-cost makes using microstructured elastomer dielectrics an excellent option for capacitive pressure sensing systems.

4. Experimental Section

Silicon Etching: The hard molds – made from <100> wafers with a 300 nm thermally grown oxide – were patterned using photolithography, and the oxide was used as a mask for the potassium hydroxide etch. The oxide was stripped using buffered hydrofluoric acid, followed by vapour deposition of tridecafluoro-1,1,2,2,-tetrahydrooctyl trichlorosilane (Gelest) to facilitate release of the mold.

Soft Mold Fabrication: To fabricate the inverted soft mold, a 10:1 mixture of PDMS elastomer (Sylgard 184, Dow Corning) to cross-linker was mixed for 2 minutes at 3000 RPM. The PDMS mixture was transferred onto the hard moulds and degassed until air bubbles were no longer present. Then the mixture was heated at 65 °C for at least 5 hours. The cross-linked PDMS above the hard mould was cut to create the inverted mould. The inverted mould was vapour treated with tridecafluoro-1,1,2,2,-tetrahydrooctyl trichlorosilane. Next, the soft mould was fabricated using the identical steps used to fabricate the inverted soft mould except the hard mould was replaced with the inverted soft PDMS mold.

Sensor Fabrication: The soft mold was mounted on a flat, rigid surface. A 5:1 mixture of PDMS elastomer to cross-linker was mixed for 2 minutes at 3000 RPM and then degassed to remove air bubbles. The PDMS mixture was transferred onto the soft mold and spin coated at 500 RPM (500 RPM/s acceleration) for 5 seconds and then immediately at 5000 RPM (1200 RPM/s acceleration) for 30 minutes. A silicon wafer coated with 90 nm aluminum was placed on the soft mould in vacuum. The stack was compressed using a 150 g weight and moved to an 80 °C oven for at least 24 hours.

Large Area Force Sensitive Trackpad: The large area sensor matrix was made using the same process, using flexible plastic PET sheets as substrates with conductive Indium Tin Oxide (ITO) electrodes arranged in a cross-bar array with the microstructures sandwiched in between. A silicon IC (Synaptics) was used to read the capacitances of each cross-point in the array and the digital information sent via serial protocol to a computer for recording.

Fingertip Pulse Sensor: An Analog Devices Inc. AD7747 capacitance-to-digital converter was used to measure the capacitance from the fingertip sensor.

Testing Stage Setup: Capacitance measurements were taken using the Agilent E4980A Precision LCR meter. Capacitances were measured at 1 kHz frequency with a 1 V a.c. signal. A mechanized z -axis stage (Newmark Systems, 0.1 μm resolution) and force gauge (Dillion GL model, 0.5 g resolution) were used to apply loads to the sensor pads on a custom-built probe station, all interfaced through a computer.

Supporting Information

Supporting Information is available from Wiley InterScience or from the author.

Acknowledgements

B.C-K.T. acknowledges support from a National Science Scholarship and the Singapore-Stanford Biodesign Global Fellowship from the Agency for Science, Technology and Research (A*STAR) and the Singapore Economic Development Board (EDB). We gratefully acknowledge P. Kallassi and P. Worfolk from Synaptics Inc. for their support and ASIC chips for capacitive readout. This research was also supported by the MSIP (Ministry of Science, ICT and Future Planning), Korea, under the "IT Consilience Creative Program" (NIPA-2014-H0201-14-1001) supervised by the NIPA (National IT Industry Promotion Agency). We also acknowledge support from the Air Force Office of Scientific Research (FA9550–12–1–0190).

Received: March 3, 2014
Revised: April 21, 2014
Published online: July 7, 2014

[1] M. L. Hammock, A. Chortos, B. C.-K. Tee, J. B.-H. Tok, Z. Bao, *Adv. Mater.* **2013**, *25*, 5997.
[2] V. J. Lumelsky, M. S. Shur, S. Wagner, *IEEE Sens. Jour.* **2001**, *1*, 41.
[3] A. N. Sokolov, B. C.-K. Tee, C. J. Bettinger, J. B.-H. Tok, Z. Bao, *Acc. Chem. Res.* **2011**, *45*, 361.
[4] E. P. Gardner, *Touch*, John Wiley & Sons, Ltd, Chichester, UK, **2010**.
[5] G. Schwartz, B. C.-K. Tee, J. Mei, A. L. Appleton, D. H. Kim, H. Wang, Z. Bao, *Nat Commun.* **2013**, *4*, 1859.
[6] C. Pang, G.-Y. Lee, T.-I. Kim, S. M. Kim, H. N. Kim, S.-H. Ahn, K.-Y. Suh, *Nat. Mater.* **2012**, *11*, 795.
[7] S. Wagner, S. P. Lacour, J. Jones, P.-H. I. Hsu, J. C. Sturm, T. Li, Z. Suo, *Physica E Low Dimens Syst Nanostruct.* **2004**, *25*, 326.
[8] T. Someya, *Stretchable Electronics*, Wiley-VCH Verlag GmbH & Co. KGaA, **2012**.
[9] B. C.-K. Tee, C. Wang, R. Allen, Z. Bao, *Nat. Nanotech.* **2012**, *7*, 1.
[10] M. Hussain, Y. Choa, *J. Mater. Sci. – Mater. Electron.* **2001**, *20*, 525.
[11] T. Someya, T. Sekitani, S. Iba, Y. Kato, H. Kawaguchi, T. Sakurai, *Proc. Natl. Acad. Sci. USA* **2004**, *101*, 9966.
[12] M. Kaltenbrunner, T. Sekitani, J. Reeder, T. Yokota, K. Kuribara, T. Tokuhara, M. Drack, R. Schwodiauer, I. Graz, S. Bauer-Gogonea, S. Bauer, T. Someya, *Nature* **2013**, *499*, 458.
[13] D.-H. Kim, R. Ghaffari, N. Lu, J. A. Rogers, *Annu. Rev. Biomed. Eng.* **2012**, *14*, 113.
[14] K. Takei, T. Takahashi, J. C. Ho, H. Ko, A. G. Gillies, P. W. Leu, R. S. Fearing, A. Javey, *Nat. Mater.* **2010**, *9*, 821.
[15] M. Zirkl, A. Sawatdee, U. Helbig, M. Krause, G. Scheipl, E. Kraker, P. A. Ersman, D. Nilsson, D. Platt, P. Bodö, S. Bauer, G. Domann, B. Stadlober, *Adv. Mater.* **2011**, *23*, 2069.
[16] S. Bauer, *IEEE Trans. Diel. Electr. Insul.* **2006**, Vol. *13*, pp. 953.
[17] C. Ohm, M. Brehmer, R. Zentel, *Adv. Mater.* **2010**, *22*, 3366.
[18] M. Ramuz, B. C.-K. Tee, J. B.-H. Tok, Z. Bao, *Adv. Mater.* **2012**, *24*, 3223.
[19] S. C. B. Mannsfeld, B. C.-K. Tee, C. V.H.-H. Chen, S. Barman, B. V. O. Muir, A. N. Sokolov, C. Reese, Z. Bao, *Nat. Mater.* **2010**, *9*, 859.
[20] C. Metzger, E. Fleisch, J. Meyer, *Appl. Phys. Lett.* **2008**, *92*, 013506.
[21] F. Schneider, T. Fellner, J. Wilde, U. Wallrabe, *J. Micromech. Microeng.* **2008**, *18*, 065008.
[22] Y. Xia, G. M. Whitesides, *Annu. Rev. Mater. Sci.* **1998**, *28*, 153.
[23] G. T. A. Kovacs, *Micromachined Transducers*, New York, McGraw-Hill, **1998**.
[24] K. Xiang, G. Huang, J. Zheng, X. Wang, G. Li, J. Huang, *J Polym Res.* **2012**, *19*, 9869.
[25] R. Stojanovic, D. Karadaglic, *Physiol. Meas.* **2007**, *28*, N19.